

THE VULNERABILITY OF HIGHLY POPULATED BUILDINGS IN THE FACE OF EARTHQUAKE AND TSUNAMI HAZARDS

Behnam Beheshtian¹, Javad Hashemi², and Hing-Ho Tsang²

¹ PhD. Candidate, Department of Civil and Construction Engineering, Swinburne University of
Technology
Melbourne, Australia
bbeheshtian@swin.edu.au

² Associate Professor, Department of Civil and Construction Engineering, Swinburne University of
Technology
Melbourne, Australia
jhashemi@swin.edu.au; htsang@swin.edu.au

Abstract

The vulnerability of highly populated buildings, such as entertainment arenas, stadiums, religious buildings, and community centres, has received little attention in the literature. These buildings are of particular concern due to their high occupancy rates and the potential for significant casualties and economic losses in the event of a natural hazard, such as an earthquake or tsunami. In this study, the AsiaWorld-Expo in Hong Kong, with a maximum capacity of over 30,000 people, was chosen as a case study. A 3D numerical model of the structure was created using the OpenSees software. A range of earthquake scenarios was used to assess the building's seismic vulnerability, whilst a physics-based methodology was utilised to generate tsunami fragility curves of the structure for a wide range of conceivable scenarios. The results of this study provide insight into the vulnerability of highly populated buildings and can lead to the development of risk-informed structural design strategies.

Keywords: Highly Populated Buildings, Earthquake Hazard, Tsunami Hazard, Fragility Curves, Risk-informed Structural Design

1. LITERATURE REVIEW

According to FEMA P-695 [1], ASCE/SEI 7-22 [2], and the International Building Code (IBC) [3], Risk Category I and II structures should have collapse probabilities of less than 10% under the maximum considered earthquake, and Risk Category III and IV structures should have collapse probabilities of 6% and 3%, respectively. Haselton et al. [4] and Liel et al. [5] compared the collapse risk of ductile and non-ductile moment frames, for which Liel and Deierlein [6] examined various seismic retrofit strategies. These studies formed the basis of the recommendations in ASCE/SEI and IBC.

Risk Category III structures, as defined by the ASCE/SEI 7-22 [2], are buildings and other structures that, if they fail, could pose a significant risk to human life. In this standard, The Risk Category IV buildings are essential facilities whose operation is critical for emergencies and defence, and their failure could pose a substantial hazard to the community. However, similar collapse risk studies have not been systematically conducted for Risk Category III and IV structures. For example, the seismic vulnerability of highly populated buildings has received limited attention in the literature. Among the few publications, Gkologiannis et al. [7] focused on the steel roof of a football stadium in Athens, Greece, and emphasised the importance of minimising its interaction with the underlying concrete structures. Uranjek et al. [8] presented necessary strengthening procedures for churches in Posočje after four significant earthquakes, and Cakir et al. [9] conducted a seismic assessment of historical masonry mosques. Dogangun and Sezen [10] investigated the seismic vulnerability of historic masonry buildings, and Sezen [11] reported on the collapse of a large proportion of masonry minarets and mosques in Düzce and Bolu after the earthquakes in 1999. Ruggieri et al. [12] developed a method for prioritising seismic risks in RC school buildings, and Zareian and Krawinkler [13] presented a probabilistic method for estimating the collapse potential of structural systems. Gholizadeh et al. [14] investigated the collapse capacity of steel concentric braced frames, Li et al. [15] used a stochastic dynamic analysis framework to understand the collapse risk of high-rise reinforced concrete structures.

Fragility analysis is a method for assessing the vulnerability of structural systems by calculating the probabilistic seismic demand, which helps reduce seismic risks through informed decision-making. Fragility curves display the conditional probability of structural demand caused by varying levels of ground shaking and can be developed using empirical or analytical methods. The collapse potential of buildings can be represented as the probability of collapse at a certain hazard level or the mean annual frequency of collapse and can be determined through the construction of a collapse fragility curve, which relates the probability of building collapse to an intensity measure such as peak ground velocity (PGV). The collapse of structural systems is defined as the maximum limit state at which one or more floor levels of the structure experience dynamic sideway instability before forming a collapse mechanism [13].

In addition to earthquakes, tsunamis are among the most devastating natural hazards due to their intensity and impact on human populations. One of the worst examples is the 2004 Indian Ocean tsunami, caused by a 9.2 magnitude undersea earthquake, which resulted in over 200,000 deaths in over ten countries. Despite Japan's extensive coastal protection infrastructure, the 2011 Great East Japan tsunami still resulted in over 15,000 deaths and \$200 billion in damages, including making several cities uninhabitable.

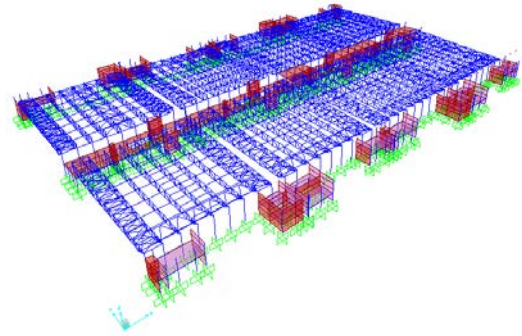
The damage caused by tsunamis on structures can be understood by relating tsunami hazards and structural vulnerability. Shuto [16] proposed a tsunami intensity defined as the logarithm of the local tsunami height to the base two. Iizuka [17] used field surveys and laboratory

experiments to determine thresholds for structural damage caused by tsunamis. An alternative approach is the use of fragility functions, which describe a structure's likelihood of going beyond a specified damage threshold according to an intensity measure such as flow depth or height. Fragility curves are typically represented by the mean and standard deviation of the cumulative lognormal distribution and are often based on empirical stochastic functions developed following tsunami events around the world (Shinozuka et al. [18] Ellingwood [19] Rosowsky and Ellingwood [20] Yuichi and Hideaki [21] Koshimura et al. [22] Park and Lindt [23]). To ensure reliable estimates of tsunami effects on the built environment, researchers such as Koshimura et al. [24] have begun developing fragility functions, which have been used in earthquake engineering for years. In order to improve tsunami mitigation plans and facilitate risk-informed decision-making, more enhanced tools are needed to predict the behaviour of structures in tsunamis.

This study attempts to fill the knowledge gap by investigating the earthquake and tsunami vulnerability of a representative highly populated building that is located along the shoreline in a region of low-to-moderate seismicity. The results will be useful for developing risk-based structural design guidelines for regions that are prone to either earthquake or tsunami hazards.

2. CASE STUDY STRUCTURE AND MODELLING

The Typical Hall Building (THB) of the AsiaWorld-Expo in Hong Kong was selected as the case study (see Figure 1). The building includes an area of approximately 70,000 m² (equivalent to 268 tennis courts) with a length of 360 meters and a width of 192 meters. The building design was originally approved based on the Hong Kong Building (Construction) Regulations 1990 and the British Standards. Structurally, it is a regular and symmetric building with columns spaced at 8.3 m along its length and two main bays, each 77 m long, across its width. In addition, the building has three stories at the centre between the B and C axes and at the far ends, with shear walls situated in the middle strip and before the A axis and after the D axis. Most walls are 20 cm thick and the top of the walls are connected to a 3D Roof-truss comprising two Mono Cap type trusses and some out-of-plan elements for lateral stability.



The Typical Hall Building

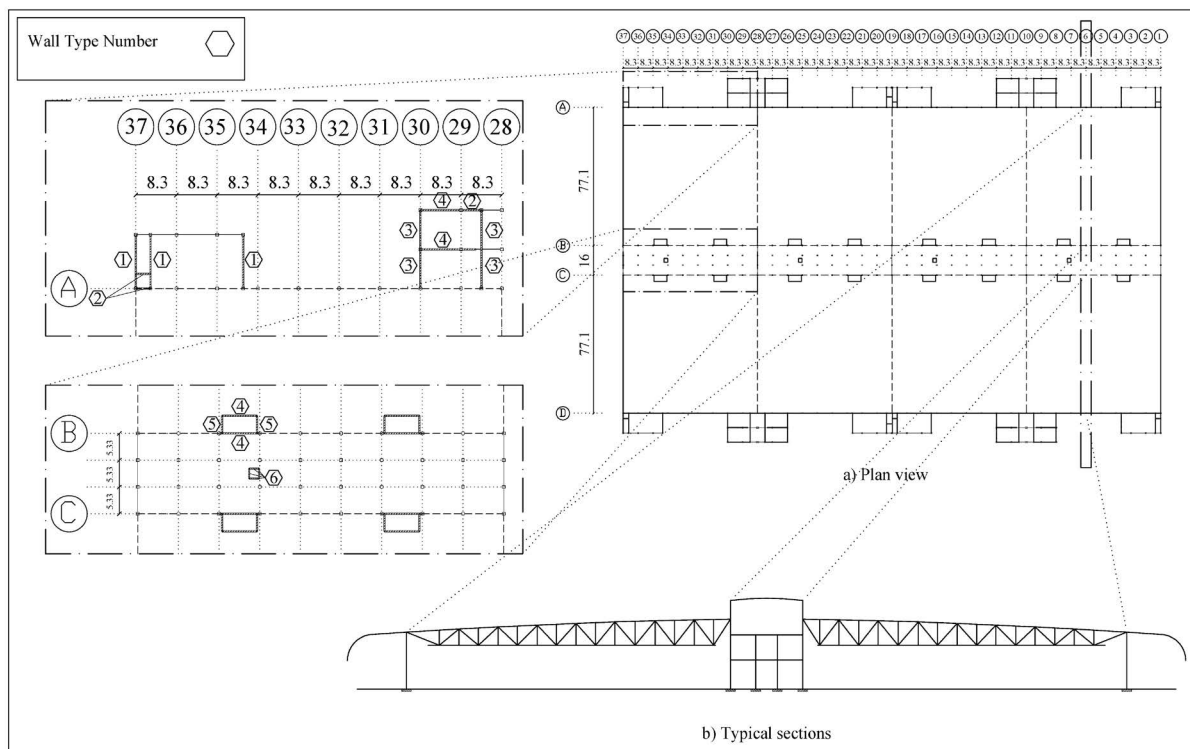


Figure 1: (a) The satellite view and (b) a 3D view of the modelled structure, (c) plan and section view of the Typical Hall Building, including shear walls, beams, and columns.

A numerical model was constructed in OpenSees [25] to perform the vulnerability analysis of the case-study structure. The utilisation of the High-Performance Computer at the Swinburne University of Technology allowed the computation time of the 3D nonlinear model of the megastructure to be reduced to a reasonable time. The OpenSeesSP 3.2.0 was used on the Linux machine for handling the analysis, and the post-processing of results was done using Matlab® [26], where a framework was designed to collect and sort the ground motion and tsunami analysis results obtained from the supercomputer and to create fragility functions. The structure was loaded based on the available instructions of the drawings, considering for each floor the self-weight, live load and dead load of 15.7 kN/m², 5 kN/m² and 2.2 kN/m², respectively. In addition to the vertical gravitational loads, the structure was subjected to lateral seismic loads, with the seismic participation mass being calculated as the dead load plus 30% of the live load. The concrete utilised in this building had a characteristic compressive strength of 40 MPa,

complying with CS1:1990, while the steel rebars had a characteristic tensile strength of 460 MPa, conforming to CS2:1995.

3. EARTHQUAKE VULNERABILITY

3.1 Damage states

Damage states are considered a fundamental part of vulnerability analysis for structures. D'Ayala et al. [27] provided a thorough overview of relevant research to assist structural engineers in developing simplified nonlinear structural models to determine structural vulnerability functions. Building-specific global performance limits of this structure are obtained from pushover curves, with definitions of the damage states and their detailed descriptions being indicated in Menegon et al. [28] and restated in other seismic guidelines and design codes such as SEAOC (1995) and ATC [29]. Further, HAZUS [30] proposed four structural damage states, including Slight, Moderate, Extensive and Complete. The slight damage is related to the effective stiffness of the structure, while Moderate damage is associated with the effective yield point where the concrete remains elastic. Extensive damage is determined at the peak strength of the lateral load-resisting system, and Complete damage is interpreted as the corresponding drift to a 20 per cent drop in post-peak strength. For the X and Y directions of the structure, drift values of 0.56, 1.2, 2.5, 4 and 0.5, 1.3, 2.8, 4 per cent are respectively considered based on the pushover analysis, the pushover curves are illustrated in Figure 2.

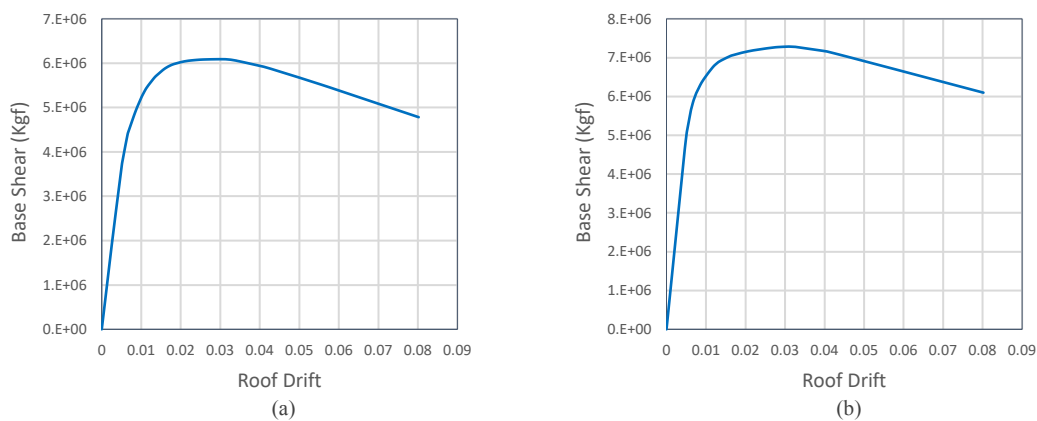


Figure 2: Pushover analysis results; (a) and (b), respectively for X and Y direction

3.2 Ground motions and fragility

Fragility assessment is an essential component of vulnerability assessment. Fragility is a probabilistic measure that predicts the level of structural damage following a seismic event. To evaluate fragility, incremental dynamic analysis (IDA) is used to determine the seismic response of a structure to a range of ground motions. This study is focused on a case study structure located in a low-to-moderate seismic zone.

For analysis, a suite of 300 ground motions was generated based on Atkinson and Boore [31] intraplate source model and the crustal properties of the region where the building is located. The ground motions were chosen based on the magnitude-distance (M-R) pairs from a study conducted on the relationship of the peak ground velocity (PGV), magnitude, and distance parameters. Major faults in the region were also included when the earthquake scenarios were

identified [28]. The outcomes of the analysis for various PGVs are analysed, and the resulting fragility curves are shown in Figure 3.

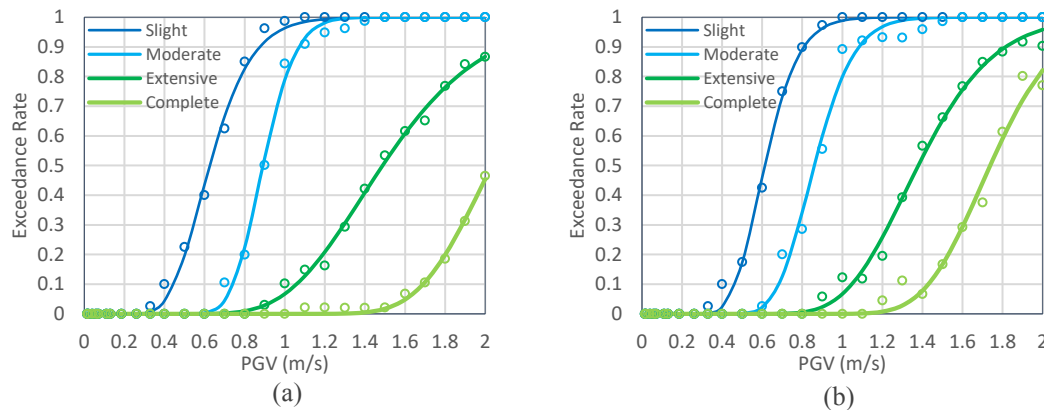


Figure 3: Seismic fragility curves based on ground motions with various magnitude-distance (M-R) combinations, (a) and (b) are respectively for X and Y directions.

4. TSUNAMI VULNERABILITY

Tsunamis are destructive natural hazard events that can lead to serious loss of life and infrastructure damage, evidenced by major disasters such as the 2004 Indian Ocean tsunami and the 2011 Great East Japan tsunami. To inform decision-makers in at-risk communities and improve tsunami mitigation plans, fragility functions have been developed that describe the likelihood of a structure exceeding a certain threshold of damage for a given intensity measure, such as flow depth or height. However, empirical fragility functions, which rely on limited data and assumptions, may not accurately reflect a structure's true vulnerability. To address this, advanced modelling approaches, such as physically-based models and hybrid models, have been proposed to generate more reliable fragility curves.

4.1 Estimation of tsunami forces

Tsunami forces can generally be broken down into five categories: hydrostatic forces, buoyant forces, hydrodynamic forces, impulsive forces, and debris impact forces [32]. Understanding these different types of forces is critical for predicting the potential impact of a tsunami on coastal structures, as well as for designing effective mitigation strategies to reduce the risk of damage and loss of life.

Hydrostatic forces result from different water depths on opposite sides of a structure. According to Heintz and Mahoney [32], the hydrostatic force of tsunami waves on a building can be calculated by the following equation:

$$F_h = \frac{1}{2} \rho_s g B h^2 \quad (1)$$

Where

ρ_s = fluid density including sediment (usually around 1200 kg/m³);

g = gravitational acceleration;

B = the width of the building in the plane normal to the flow direction;

h = water height above the base of the wall;

Hydrodynamic forces, which are generated by the water flow at moderate to high velocities, can be determined from the equation:

$$F_d = \frac{1}{2} \rho_s C_d B (hu^2)_{max} \quad (2)$$

Where

C_d = coefficient of drag;

B = width of the building in the plane normal to the flow direction;

h = flow depth;

u = flow velocity

Finally, the total lateral dynamic force on the structure is calculated by the equation:

$$F_d = \frac{1}{2} \rho_s C_d B C_0 (hu^2)_{max} \quad (3)$$

Where

C_0 = deamplifying coefficient to account for openings and wall/window failure/breakage. Which is suggested to have a value greater than 0.7 [33].

4.2 Proposed Methodology

The Monte Carlo Simulation is employed to calculate tsunami forces and generate fragility curves. The maximum flow depth of 9 m is chosen based on the maximum observed height during the 2004 Indian Ocean tsunami [34]. The dimensionless Froude number of 2 is applied as a constraint to consider only combinations of flow depths and velocities that have a historical reminiscence. For each set of tsunami forces, 50 random combinations of drag coefficient and deamplifying coefficient are used to calculate the total tsunami force and generate an array of possible outcomes. Structural performance is evaluated by considering inter-story drifts as the engineering demand parameter. By performing a pushover analysis of the structure for each tsunami load case, the maximum inter-story drifts are compared with the four aforementioned limit states, and the structure's performance for that particular case is achieved. The exceedance probability of each limit state is calculated, and fragility curves are plotted.

Flow depth is the most popular intensity measure within the tsunami research literature, and physics-based fragility curves can be developed using this intensity measure. However, this intensity measure may not be the most accurate due to different forces that can be imposed on the structure with the same heights and various velocities. The momentum flux is introduced to improve on this as a better intensity measure. Momentum flux is an essential measure in fluid mechanics that quantifies the transfer of momentum by a fluid. In tsunami fragility analysis, momentum flux is a preferred intensity measure, representing a more accurate estimation of the hydrodynamic forces resulting in structural damage [35]. The momentum flux can be calculated by combining the flow depth and velocity (hu^2). However, for considering various scenarios, the accuracy of the results is highly dependent on the increment values chosen for each parameter. To overcome this, momentum flux itself is incremented, resulting in a more precise representation of the tsunami forces. The fragility curves developed with momentum flux as an intensity measure provide a more accurate representation of a tsunami's impact on structures

compared to those based solely on flow depth. This improved accuracy is primarily attributed to the inclusion of velocity in the realisation of tsunami action. The resulting fragility curves for the case study structure based on flow depth and momentum flux are plotted in Figure 4.

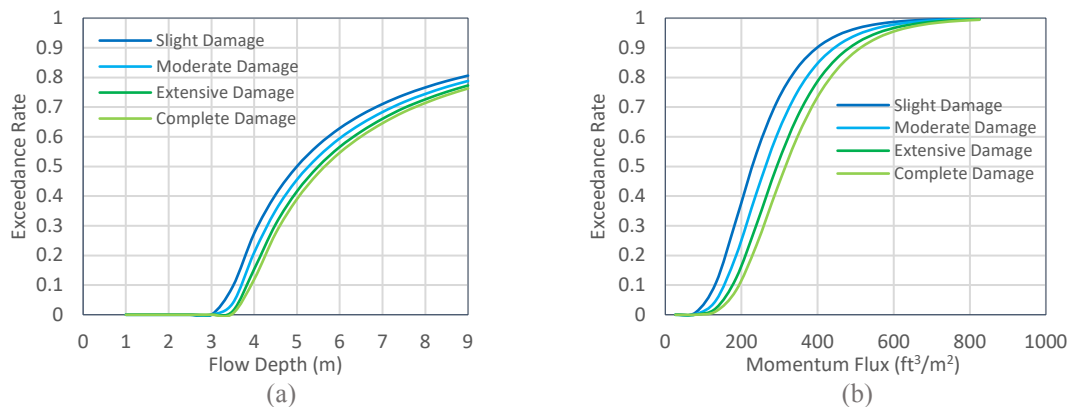


Figure 4: Fragility curves (a) and (b) for tsunamis are based on intensity measures of flow depth and momentum flux, respectively. These curves represent the exceedance rate of four damage states: slight, moderate, extensive, and complete.

In Figure 4 (a), there is a narrow band between the various limit state rates. This narrow band indicates that the flow depth may not be the most effective intensity measure for evaluating the tsunami performance of structures. For example, in a scenario where a tsunami with a height of 5 meters occurs, the probability of slight damage is 50 per cent, while the probability of complete damage is 40 per cent. This suggests the inadequacy of the flow depth as an intensity measure in distinguishing between the different severity levels of tsunamis and its lack of sensitivity. Figure 4 (b) displays momentum flux, which provides a more accurate representation of the various states of a structure's response, making it a better measure for evaluating the intensity of tsunamis. Therefore, momentum flux is a preferable alternative to flow depth for assessing the tsunami performance of structures.

5. CONCLUSIONS AND CLOSING REMARKS

In this study, the focus was on the vulnerability of buildings with high occupancy number. The AsiaWorld-Expo in Hong Kong was used as a case study. A 3D numerical model was created using OpenSees software to assess its seismic vulnerability in various earthquake scenarios. Using the developed model and by incorporating a Physics-based methodology, the tsunami response of the structure in various tsunami scenarios was determined. Lastly, the fragility curves of the structure were generated.

According to Figure 2, the structure under investigation is more vulnerable in the Y direction compared to the X direction. This is due to the presence of fewer shear walls in the Y direction, which has consequently resulted in a higher rate of complete damage. To have a notion of the risk that this building can impose on its residents, the concept of individual risk, as described in previous studies [36, 37], should be taken into account. Next, the number of casualties (N) should be defined as a function of the area of collapsed columns (A_{col}), based on Tanner and Hingorani [38]. As a result, the estimated number of casualties for this building in case of losing one column would be around 14 individuals. Finally, by looking at the fragility curves, it can be realised that in an earthquake with a peak ground velocity (PGV) of 1.4 m/s, the collapse probability would be 10%. Thus, by multiplying the estimated number of casualties with the

probability of collapse, the median probability of the number of casualties would be 1.4 persons under a high PGV of 1.4 m/s.

Regarding the tsunami hazard, as shown in Figure 4, the behaviour of the structure changes significantly as the height of the tsunami increases. The structure is insensitive to low-height tsunamis due to its strong lateral stiffness and the imposed Froude number on the calculation of tsunami forces. The Froude number limits the velocity of the water to a certain value, which, in turn, limits the load that can be applied to the structure. However, when the height of the tsunami increases, the maximum attainable velocity also increases. This combined effect of tsunami height and increased velocity leads to a greater lateral force on the structure.

In evaluating the impact of tsunamis on structures, momentum flux appeared to be a more appropriate intensity measure than flow depth. This is because momentum flux provides a more accurate estimation of hydrodynamic forces and is more sensitive to the severity of tsunamis. Fragility curves based on momentum flux also offer a more precise representation of tsunami impact, making it a preferable alternative to flow depth.

As discussed above, the results have provided insights into the vulnerability of high occupancy buildings in the face of earthquake and tsunami actions and can be used to inform the development of risk-informed design strategies.

References

- [1] ATC, *Quantification of building seismic performance factors*. US Department of Homeland Security, FEMA, 2009.
- [2] ASCE7-22, *ASCE/SEI Minimum Design Loads for Building and Other Structures ASCE/SEI 7-10*. American Society of Civil Engineers, 2022.
- [3] U. B. Code, "International building code," *International Code Council, USA*, 1997.
- [4] C. B. Haselton, A. B. Liel, G. G. Deierlein, B. S. Dean, and J. H. Chou, "Seismic Collapse Safety of Reinforced Concrete Buildings. I: Assessment of Ductile Moment Frames," *Journal of Structural Engineering*, vol. 137, no. 4, pp. 481-491, 2011, doi: 10.1061/(asce)st.1943-541x.0000318.
- [5] A. B. Liel, C. B. Haselton, and G. G. Deierlein, "Seismic collapse safety of reinforced concrete buildings. II: Comparative assessment of nonductile and ductile moment frames," *Journal of Structural Engineering*, vol. 137, no. 3, pp. 492-502, 2011.
- [6] A. B. Liel and G. G. Deierlein, "Cost-Benefit Evaluation of Seismic Risk Mitigation Alternatives for Older Concrete Frame Buildings," *Earthquake Spectra*, vol. 29, no. 4, pp. 1391-1411, 2013, doi: 10.1193/030911eqs040m.
- [7] C. Gkologianis, C. Gantes, A. Athanasiadis, M. Majowiecki, F. Zoulas, and H. Schmidt, "Structural Design of the New Football Stadium of Panathinaikos F.C. in Votanikos, Greece," *IABSE Symposium Report*, vol. 97, no. 34, pp. 63-70, 2010, doi: 10.2749/222137810796024097.
- [8] M. Uranjek, B. Dolinšek, and S. Gostič, "Seismic strengthening of churches as a part of earthquake renewal in the Posočje region, Slovenia," 2011: WIT Press, doi: 10.2495/eres110201. [Online]. Available: <https://dx.doi.org/10.2495/eres110201>
- [9] F. Cakir, B. S. Seker, A. Durmus, A. Dogangun, and H. Uysal, "Seismic assessment of a historical masonry mosque by experimental tests and finite element analyses," *KSCSE Journal of Civil Engineering*, vol. 19, no. 1, pp. 158-164, 2015, doi: 10.1007/s12205-014-0468-4.
- [10] A. Dogangun and H. Sezen, "Seismic vulnerability and preservation of historical masonry monumental structures," *Earthquakes and Structures*, vol. 3, no. 1, pp. 83-95, 2012, doi: 10.12989/eas.2012.3.1.083.
- [11] H. Sezen, *Earthquake Engineering*. 2012.
- [12] S. Ruggieri, D. Perrone, M. Leone, G. Uva, and M. A. Aiello, "A prioritization RVS methodology for the seismic risk assessment of RC school buildings," *International Journal of Disaster Risk Reduction*, vol. 51, p. 101807, 2020/12/01/ 2020, doi: <https://doi.org/10.1016/j.ijdr.2020.101807>.
- [13] F. Zareian and H. Krawinkler, "Assessment of probability of collapse and design for collapse safety," *Earthquake Engineering & Structural Dynamics*, vol. 36, no. 13, pp. 1901-1914, 2007.
- [14] S. Gholizadeh, A. Hassanzadeh, A. Milany, and H. F. Ghatte, "On the seismic collapse capacity of optimally designed steel braced frames," *Engineering with Computers*, vol. 38, no. 2, pp. 985-997, 2022/04/01 2022, doi: 10.1007/s00366-020-01096-7.
- [15] J. Li, H. Zhou, and Y. Ding, "Stochastic seismic collapse and reliability assessment of high-rise reinforced concrete structures," *The Structural Design of Tall and Special Buildings*, vol. 27, no. 2, p. e1417, 2018.
- [16] N. Shuto, "Tsunami intensity and disasters," in *Tsunamis in the World*: Springer, 1993, pp. 197-216.
- [17] H. Iizuka, "Damage due to the flooding flow of tsunami," in *Proceedings of Coastal Engineering, JSCE*, 2000, vol. 47, pp. 381-385.

- [18] M. Shinozuka, M. Q. Feng, J. Lee, and T. Naganuma, "Statistical Analysis of Fragility Curves," *Journal of Engineering Mechanics*, vol. 126, no. 12, pp. 1224-1231, 2000, doi: doi:10.1061/(ASCE)0733-9399(2000)126:12(1224).
- [19] B. R. Ellingwood, "Earthquake risk assessment of building structures," *Reliability Engineering & System Safety*, vol. 74, no. 3, pp. 251-262, 2001.
- [20] D. V. Rosowsky and B. R. Ellingwood, "Performance-Based Engineering of Wood Frame Housing: Fragility Analysis Methodology," *Journal of Structural Engineering*, vol. 128, no. 1, pp. 32-38, 2002, doi: doi:10.1061/(ASCE)0733-9445(2002)128:1(32).
- [21] N. Yuichi and Y. Hideaki, *Journal of Disaster Research* VL - 4 IS - 6 SP - 479 EP - 488 PY - 2009 DO - 10.20965/jdr.2009.p0479 ER -.
- [22] S. Koshimura, T. Oie, H. Yanagisawa, and F. Imamura, "Developing Fragility Functions for Tsunami Damage Estimation Using Numerical Model and Post-Tsunami Data from Banda Aceh, Indonesia," *Coastal Engineering Journal*, vol. 51, no. 3, pp. 243-273, 2009/09/01 2009, doi: 10.1142/S0578563409002004.
- [23] S. Park and J. W. v. d. Lindt, "Formulation of Seismic Fragilities for a Wood-Frame Building Based on Visually Determined Damage Indexes," *Journal of Performance of Constructed Facilities*, vol. 23, no. 5, pp. 346-352, 2009, doi: doi:10.1061/(ASCE)CF.1943-5509.0000034.
- [24] S. Koshimura, Y. Namegaya, and H. Yanagisawa, "Tsunami fragility: A new measure to identify tsunami damage," *Journal of Disaster Research*, vol. 4, no. 6, pp. 479-488, 2009.
- [25] S. Mazzoni, F. McKenna, M. H. Scott, and G. L. Fenves, "OpenSees command language manual," *Pacific Earthquake Engineering Research (PEER) Center*, 2006.
- [26] *MATLAB:2019a*. (2019). The MathWorks Inc.
- [27] D. D'Ayala, A. Meslem, D. Vamvatsikos, K. Porter, T. Rossetto, and V. Silva, "Guidelines for analytical vulnerability assessment of low/mid-rise buildings, vulnerability global component project," *Global Earthquake Model*, 2015.
- [28] S. J. Menegon, H. H. Tsang, E. Lumantarna, N. T. K. Lam, J. L. Wilson, and E. F. Gad, "Framework for seismic vulnerability assessment of reinforced concrete buildings in Australia," *Australian Journal of Structural Engineering*, vol. 20, no. 2, pp. 143-158, 2019/04/03 2019, doi: 10.1080/13287982.2019.1611034.
- [29] ATC, "Preliminary Evaluation of Methods for Defining Performance, ATC-58-2," ed: Applied Technology Council, 2003.
- [30] F. HAZUS, "2.1 technical manual," Technical report, Federal Emergency Management Agency, 2012.
- [31] G. M. Atkinson and D. M. Boore, "Earthquake Ground-Motion Prediction Equations for Eastern North America," *Bulletin of the Seismological Society of America*, vol. 96, no. 6, pp. 2181-2205, 2006, doi: 10.1785/0120050245.
- [32] J. Heintz and M. Mahoney, "Guidelines for design of structures for vertical evacuation from tsunamis," *FEMA P646/June*, 2008.
- [33] H. Fukuyama *et al.*, "Structural design requirement on the tsunami evacuation buildings," *UJNR, Tokyo*, 2011.
- [34] J. Goff *et al.*, "Sri Lanka field survey after the December 2004 Indian Ocean tsunami," *Earthquake Spectra*, vol. 22, no. 3_suppl, pp. 155-172, 2006.
- [35] H. Park, D. M. Wiebe, D. T. Cox, and K. Cox, "Tsunami Inundation Modeling: Sensitivity of Velocity and Momentum Flux to Bottom Friction with Application to Building Damage at Seaside, Oregon," *Coastal Engineering Proceedings*, vol. 1, no. 34, p. 1, 2014, doi: 10.9753/icce.v34.currents.1.

- [36] H.-H. Tsang and F. Wenzel, "Setting structural safety requirement for controlling earthquake mortality risk," *Safety Science*, vol. 86, pp. 174-183, 2016/07/01/ 2016, doi: <https://doi.org/10.1016/j.ssci.2016.02.028>.
- [37] R. D. Steenbergen, M. Sýkora, D. Diamantidis, M. Holický, and T. Vrouwenvelder, "Economic and human safety reliability levels for existing structures," *Structural Concrete*, vol. 16, no. 3, pp. 323-332, 2015.
- [38] P. Tanner and R. Hingorani, *Development of Risk-Based Requirements for Structural Safety*. 2010.